Pergamon

Int. J. Heat Mass Transfer. Vol. 38, No. 18, pp. 3413–3421, 1995

0017–9310/95 $9.50 + 0.00

0017–9310(95)00071–2

Effect of the temperature dependence of fluid properties on the migration of an interface in double-diffusive natural convection

KATSUYOSHI KAMAKURA
Toyama National College of Technology, 13 Hongo-machi, Toyama 939, Japan

and

HIROYUKI OZOE†
Institute of Advanced Material Study, Kyushu University, 6–1 Kasuga-koen, Kasuga 816, Japan

(*Received* 30 *May* 1994 *and in final form* 2 *February* 1995)

Abstract—Experimental observation has shown that a slightly tilted sharp interface between two convection layers in double-diffusive natural convection migrates perpetually upward gradually with time. This movement of an interface cannot be explained by a simple mathematical model of constant physical properties. The present paper studies the numerical analyses of two-layer convection with the temperature dependence of the properties of the fluid. The perpetual upward migration of an interface was found to be promoted mainly by the temperature dependence of the volumetric coefficient of thermal expansion and also by that of the kinematic viscosity. However, the diffusion coefficient was independent of the migration. The upward migration of an interface appears to be caused by the difference between the intensity of etching due to the flow along the hot wall in the lower layer and that along the cold wall in the upper layer.

1. INTRODUCTION

Natural convection in which the buoyant forces are due both to temperature and concentration gradients is generally referred to as double-diffusive convection. In double-diffusive convection, multi-layered roll cells are mostly formed and then slightly tilted sharp interfaces are observed. The solute in the double-diffusive natural convection is transferred generally from below to above the interfaces, but thermal energy is transferred either vertically or laterally depending on the boundary conditions. The system heated from below was first studied by oceanographers, and the first example in the literature appears to be the experiment of Turner and Stommel [1]. Turner and co-workers developed the study of double-diffusive convection as described in a number of reviews [2–4]. The system heated laterally produces stable multi-layered convection [5, 6]. For example, when a solution having a concentration gradient along the gravitational direction is heated from one vertical side wall and cooled from an opposing wall, multi-layered roll cells are formed and slightly tilted sharp interfaces are observed. Detailed observation of the interfaces suggests that there is a migration of interfaces between two convection layers as described in our previous paper [7]. All interfaces have a tendency to migrate perpetually upward gradually with time, but the corresponding numerical analyses for multi-layered convection failed to simulate this migration of the interfaces. This curious upward migration is studied by the present numerical model for two-layer convection with the temperature dependence of the physical properties of the fluid.

A simple model for double-diffusive natural convection is a two-layer convection as shown in Fig. 1. It consists of water (upper layer) and an aqueous solution (lower layer). Both layers are heated from one side and cooled from the opposite side, and convection starts in each layer. The volumes of the upper and lower layers are the same at the start of convection. The system is symmetric with respect to a central vertical plane at $X = 0.25$, since the top of the system is a free surface and the bottom is a fixed wall. Similarly to the case of multi-layered convection, the corresponding simple numerical analyses for this two-layer system failed to simulate the migration of an interface [8, 9]. However, the experimental observation represented the unsymmetrical upward migration of an interface as time proceeds after a step heating and cooling of the vertical walls, as shown in Fig. 2 for a system of KCl solution and water [9, 10]. The present paper tries to simulate this migration of the interface with mathematical model equations as described below.

†Author to whom correspondence should be addressed.

NOMENCLATURE

A	aspect ratio, $2H/B$
B	horizontal width of a solution layer
C	dimensionless concentration, $(c-c_0)/\Delta c_{max}$
c	concentration
c_{max}	initial maximum concentration (initial concentration of a lower layer)
c_{min}	initial minimum concentration (initial concentration of an upper layer)
c_0	$(c_{max}+c_{min})/2$
D	diffusion coefficient
d	dimensionless density (specific gravity)
$\mathbf{g}$	acceleration due to gravity
H	initial height of the upper layer or the lower layer
Le	Lewis number, κ/D
N	buoyancy ratio, $\beta\Delta c_{max}/(\alpha\Delta T_{max})$
Nu_{loc}	local Nusselt number
Pr	Prandtl number, ν/κ
Ra	Rayleigh number, $g\alpha\Delta T_{max}H^3/(\kappa\nu)$
T	temperature
T_{cold}	temperature on the cold wall
T_{hot}	temperature on the hot wall
T_0	$(T_{hot}+T_{cold})/2$
t	time
U	dimensionless velocity, $\mathbf{u}H/\kappa$
$\mathbf{u}$	velocity in the x direction
V	dimensionless velocity, $\mathbf{v}H/\kappa$
$\mathbf{V}_{max}$	maximum $\mathbf{V}$ at $Y=0.5$ or 1.5
$\mathbf{v}$	velocity in the y direction
X	dimensionless coordinate, x/H
x	horizontal coordinate
Y	dimensionless coordinate, y/H
y	vertical coordinate.

Greek symbols

α	volumetric coefficient of expansion with temperature
β	volumetric coefficient of expansion with concentration
Δc_{max}	$c_{max}-c_{min}$
ΔT_{max}	$T_{hot}-T_{cold}$
$\Delta\tau$	dimensionless time step
ζ	dimensionless vorticity
θ	dimensionless temperature, $(T-T_0)/\Delta T_{max}$
κ	thermal diffusivity
ν	kinematic viscosity
τ	dimensionless time
ψ	dimensionless stream-function $(U=\partial\psi/\partial Y,\ V=-\partial\psi/\partial X)$
ω	vorticity.

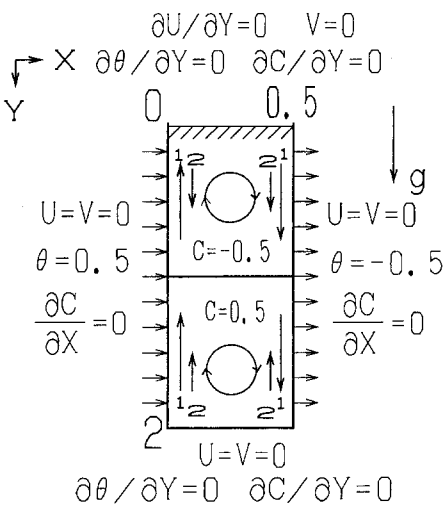

Fig. 1. Schematic illustration of two-layer convection and boundary conditions. 1: buoyancy due to temperature difference, 2: buoyancy due to concentration difference.

2. ANALYSIS

2.1. *Mathematical model*

The basic equations [11] to describe double-diffusive natural convection consist of the stream-function equation, the vorticity equation, the energy equation and the concentration equation as follows in dimensionless forms:

$$\zeta=\frac{\partial V}{\partial X}-\frac{\partial U}{\partial Y}=-\nabla^2\psi \tag{1}$$

$$\frac{\partial\zeta}{\partial\tau}+U\frac{\partial\zeta}{\partial X}+V\frac{\partial\zeta}{\partial Y}=Pr\,Ra\left(-\frac{\partial\theta}{\partial X}+N\frac{\partial C}{\partial X}\right)+Pr\nabla^2\zeta \tag{2}$$

$$\frac{\partial\theta}{\partial\tau}+U\frac{\partial\theta}{\partial X}+V\frac{\partial\theta}{\partial Y}=\nabla^2\theta \tag{3}$$

$$\frac{\partial C}{\partial\tau}+U\frac{\partial C}{\partial X}+V\frac{\partial C}{\partial Y}=\nabla^2C/Le. \tag{4}$$

Dimensionless parameters Pr, Ra, Le, N and A are defined as follows.

$$Pr=\frac{\nu}{\kappa}\quad Ra=\frac{g\alpha\Delta T_{max}H^3}{\kappa\nu}\quad Le=\frac{\kappa}{D}$$

$$N=\frac{\beta\Delta c_{max}}{\alpha\Delta T_{max}}\quad A=\frac{2H}{B}. \tag{5}$$

Here, the dimensionless variables are defined as follows.

$$X=x/H\quad Y=y/H\quad U=uH/\kappa$$

$$V=vH/\kappa\quad \tau=t\kappa/H^2\quad \zeta=\omega H^2/\kappa$$

$$\theta=(T-T_0)/\Delta T_{max}\quad C=(c-c_0)/\Delta c_{max}. \tag{6}$$

2.2. *Temperature dependence of fluid properties*

The properties of fluid to affect the double-diffusive natural convection are volumetric coefficient of ther-

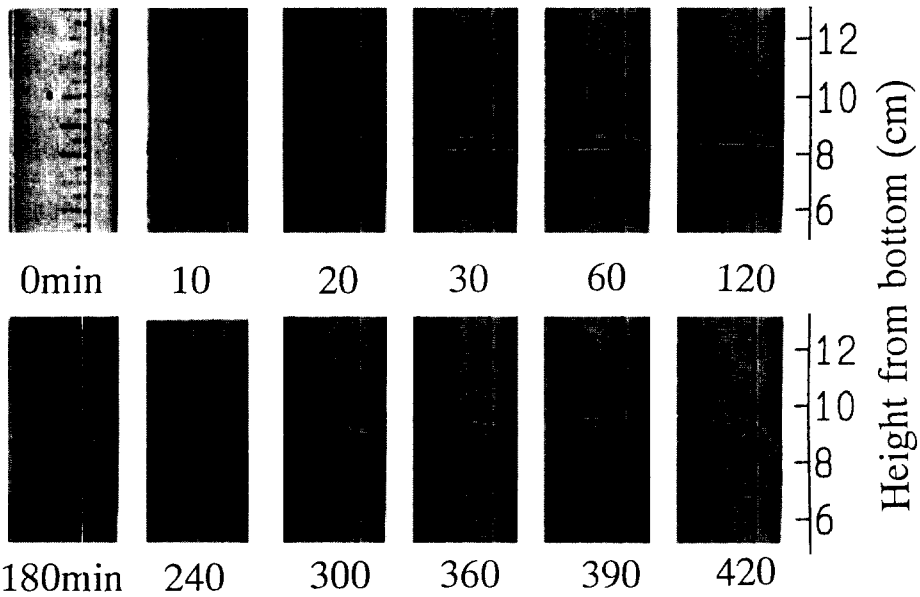

Fig. 2. Shadowgraphs of interface between layers. The time is the elapsed time from the start of heating and cooling. The experimental apparatus and conditions are the same as those described in the literature [10]. Initial upper layer: water (8 cm in height); initial lower layer: 10 kg m^{-3} KCl (8 cm in height); heating: 30°C (left-hand side); cooling: 20°C (right-hand side). The above experimental conditions can be summarized as follows: $Pr = 6.27$, $Le = 71.8$, $A = 4$, $N = 2.74$ and $Ra = 9.23 \times 10^7$.

mal expansion (α), volumetric coefficient of expansion with concentration (β), kinematic viscosity (ν), thermal diffusivity (κ) and diffusion coefficient (D), in which α, ν or D depend largely on temperature (see Fig. 3) but β and κ are not so dependent. Then it is apparent from the definition of dimensionless parameters given in equation (5) that Pr is proportional to ν, $Pr\,Ra$ is proportional to α, N is inversely proportional to α and that Le is inversely proportional to D. In Fig. 3 the relation between the property of fluid and temperature is roughly linear for ν and D, but slightly curved for α. Then the dimensionless parameters are expressed by the following equations:

$$Pr = Pr_0(1+a_1\theta) \tag{7}$$

$$Pr\,Ra = Pr_0 Ra_0(1+a_2\theta+a_3\theta^2) \tag{8}$$

$$N = N_0(1+a_4\theta+a_5\theta^2)^{-1} \tag{9}$$

$$Le = Le_0(1+a_6\theta)^{-1}. \tag{10}$$

For example, the coefficients for the properties of water at 25°C ($T_{hot} = 30$°C and $T_{cold} = 20$°C) are as follows:

$$a_1 = -0.226$$

$$a_2 = a_4 = 0.292$$

$$a_3 = a_5 = -0.087$$

$$a_6 = 0.260.$$

Here the diffusion coefficient is assumed to be the value for diluted KCl in water.

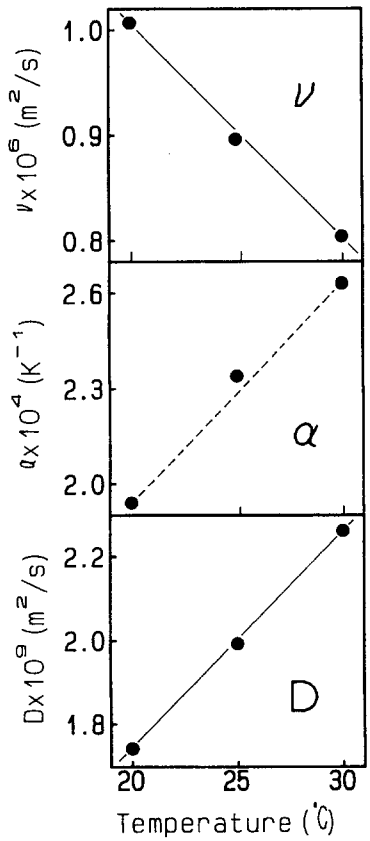

Fig. 3. Temperature dependence of the properties of the fluid.

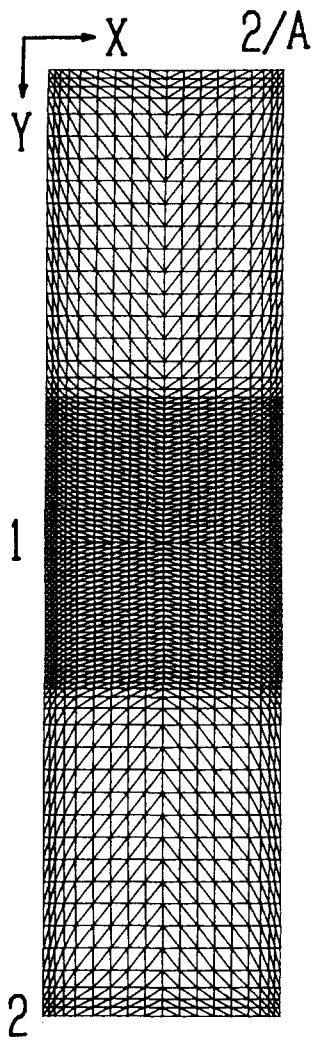

Fig. 4. Finite element mesh with 1691 nodes and 3168 elements.

2.3. *Numerical analysis*

The model equations were numerically solved by the finite element method for the two-layer convection. The calculation of finite element method was carried out by the same algorithm as that used in our previous paper [11], except for the temperature dependence. Figure 4 shows the finite element meshes in which fine meshes are employed in the vicinity of a horizontal central height ($Y = 1$). Then stable numerical simulations could be carried out for the migration of an interface. The coordinates of division are as follows:

$$164X = 0, 2, 4, 7, 11, 17, 23, 29, 35, 41, 47, 53, 59, 65, 71, 75, 78, 80, 82$$

$$169Y = 0, 3, 6, 10, 16, \ldots (\text{difference} = 8)\ldots, 104, 110, 114, 117, \ldots (\text{difference} = 2)\ldots, 221, 224, 228, 234, \ldots (\text{difference} = 8)\ldots, 322, 328, 332, 335, 338.$$

The mesh for the present computation is 1691 nodes and 3168 elements, which is finer than the 1311 node and 2448 elements used in the previous simulation of the two-layer convection [9].

The boundary conditions in dimensionless form are given as follows (see Fig. 1):

$$\text{at } Y = 0: \quad \partial U/\partial Y = 0, V = 0, \partial\theta/\partial Y = 0, \partial C/\partial Y = 0$$

$$\text{at } Y = 2: \quad U = V = 0, \partial\theta/\partial Y = 0, \partial C/\partial Y = 0$$

$$\text{at } X = 0: \quad U = V = 0, \theta = 0.5, \partial C/\partial X = 0$$

$$\text{at } X = 0.5: \quad U = V = 0, \theta = -0.5, \partial C/\partial X = 0.$$

The initial concentration in the system is $+0.5$ in the lower layer and -0.5 in the upper layer.

Computations were carried out for $Pr_0 = 6$, $Le_0 = 100$, $A = 4$, $N_0 = 2$ and $Ra_0 = 10^5$. These correspond roughly to the experimental values as mentioned in the caption of Fig. 2, except for the Rayleigh number. The computation with the Rayleigh number at $Ra_0 = 10^7$ in accordance with the experimental value did not converge with the current element numbers. Stable computation appears to require much finer element sizes, which is not possible with our current computer resources. Although the present computation is limited to being 100 times smaller than the experimental correspondence, the qualitative characteristics are expected to hold even at higher Rayleigh numbers. In the experiments with Rayleigh number two orders lower it was difficult to keep the temperature difference between the hot and cold walls at a constant small value such as 0.1 K.

The effect of the temperature dependence of fluid properties on the migration was studied for the five different cases as follows.

Case 1: no temperature dependence

$$a_1 = a_2 = a_3 = a_4 = a_5 = a_6 = 0.$$

Case 2: temperature dependence of α, ν and D

$$a_1 = -0.226, \quad a_2 = a_4 = 0.292,$$

$$a_3 = a_5 = -0.087, \quad a_6 = 0.260.$$

Case 3: temperature dependence of α

$$a_1 = 0, \quad a_2 = a_4 = 0.292,$$

$$a_3 = a_5 = -0.087, \quad a_6 = 0.$$

Case 4: temperature dependence of ν

$$a_1 = -0.226, \quad a_2 = a_4 = 0, \quad a_3 = a_5 = 0, \quad a_6 = 0.$$

Case 5: temperature dependence of D

$$a_1 = 0, \quad a_2 = a_4 = 0, \quad a_3 = a_5 = 0, \quad a_6 = 0.260.$$

The calculations were carried out on an HP Apollo 9000 Model 710.

3. RESULTS

3.1. *Two-layer convection phenomenon*

Figure 5 shows the instantaneous contours of stream function and concentration for the system with temperature dependence of α, ν and D (case 2). At first the contour of stream function gives two roll cells of the same size. However, the lower roll cell becomes larger gradually with time and then the upper roll cell smaller. This characteristic differs from that obtained without considering the temperature dependence of properties, as described in previous papers [8, 9], where the sizes of two roll cells were the same over a long period of time. The contours of concentration in Fig. 5 correspond to those of the stream function. Namely the lower layer becomes larger gradually with time. The computation was quit at $\tau = 2.4$ because of the change to a single roll.

Figure 6 shows the height $(2-Y)$ of the interface at the center of the enclosure (at $X = 0.25$) vs time. In the case of no temperature dependence, the interface represented by black circle is at a central height with some fluctuation. In the case of the temperature dependence of α, ν and D, the interface represented by open circles moves noticeably upward with time. This means that the temperature dependence of the properties of fluid is related to the migration of the interface. When the temperature dependence of α (black square) or ν (open triangle) exists, the interface moves upward with time and then the interface for α moves faster than that for ν. When the temperature dependence of D (open square) exists, the interface is at rest. Actually, all physical properties depend on the temperature and the transient movement of the interface represented by open circles is most plausible in a real experiment.

3.2. *Fluid velocity near the walls*

The migration of an interface may be caused by the etching due to the flow against the interface. Figure 7 shows the vertical velocity profiles at $Y = 1/2$ (mid height in an upper layer) and at $Y = 3/2$ (mid height in a lower layer). In the case of no temperature dependence (case 1), the maximum absolute velocity near the hot wall in the lower layer is almost equal to that near the cold wall in the upper layer. The small difference is because of the free upper surface and rigid bottom wall. On the other hand, when we consider the temperature dependence in α, ν and D (case 2), the maximum absolute velocity near the hot wall hitting the interface from the lower layer is much higher than that near the cold wall in the upper layer hitting the interface downward. The flow velocity near the hot wall is more vigorous than the flow near the cold wall. The vigorous flow along the hot wall in the lower layer collides with the interface, and similarly that along the cold wall in the upper layer also collides with the interface. The difference in the inertial force between two flows should be a driving force for the migration of an interface. Namely the inertial force to hit the interface may be more persuasive for the movement of the interface: to assess this another graph is prepared as shown in Fig. 8. The ordinate represents the dimensionless inertial force $F(= dV_{\max}^2)$ for case 1 and case 2. The dimensionless inertial force was defined by the following equation.

$$F = dV_{\max}^2 = \left(1 - \frac{\beta \Delta c_{\max}}{N}\theta + \alpha \Delta T_{\max} NC\right) V_{\max}^2. \tag{11}$$

For the case of no temperature dependence of physical properties (case 1), the inertial forces at $Y = 0.5$ and 1.5 represented by solid lines are almost the same magnitude. On the other hand, for the case of temperature dependence of physical properties (case 2), the inertial forces represented by dotted lines give a large difference in their magnitude. The maximum inertial force at $Y = 1.5$ and $\tau = 0.9$ for the upward flow along the heated wall towards the interface from the lower layer, as shown by a bold dashed line, is $F = 5946$ in contrast to that as shown by a fine dashed line, $F = 3451$, which is at $Y = 0.5$ and $\tau = 0.9$ for the downward flow along the cold wall towards the interface from the upper layer. This large difference in the magnitude in the inertial force of fluid to hit the interface could be responsible for the upward movement of the interface.

Figure 9 shows a number of instantaneous vertical profiles of the local Nusselt number on the hot wall for the case of the temperature dependence in α, ν and D (case 2). The peaks of local Nusselt number near the bottom of the lower layer are higher than those in the upper layer; this is due to the difference in the boundary condition at the lower plane in each convection layer and is similar to that with no temperature dependence as shown in the previous papers [8, 9]. However, the peak in the upper layer moves upward and becomes low. This means that the heat transfer rate in the upper layer becomes weaker with time than that in the lower layer with decrease in the size of the upper layer.

4. CONCLUSIONS

The migration of an interface for two-layer convection is successfully computed with the temperature dependence of the properties of the fluid. The migration of an interface is affected by the temperature dependence of properties as follows.

(1) The volumetric coefficient of thermal expansion (α) contributes to the fastest upward migration.
(2) The kinematic viscosity (ν) also contributes to the upward migration.
(3) The diffusion coefficient (D) does not contribute to the migration.

The migration of an interface is caused by the etching rate in the flow along the hot wall in the lower

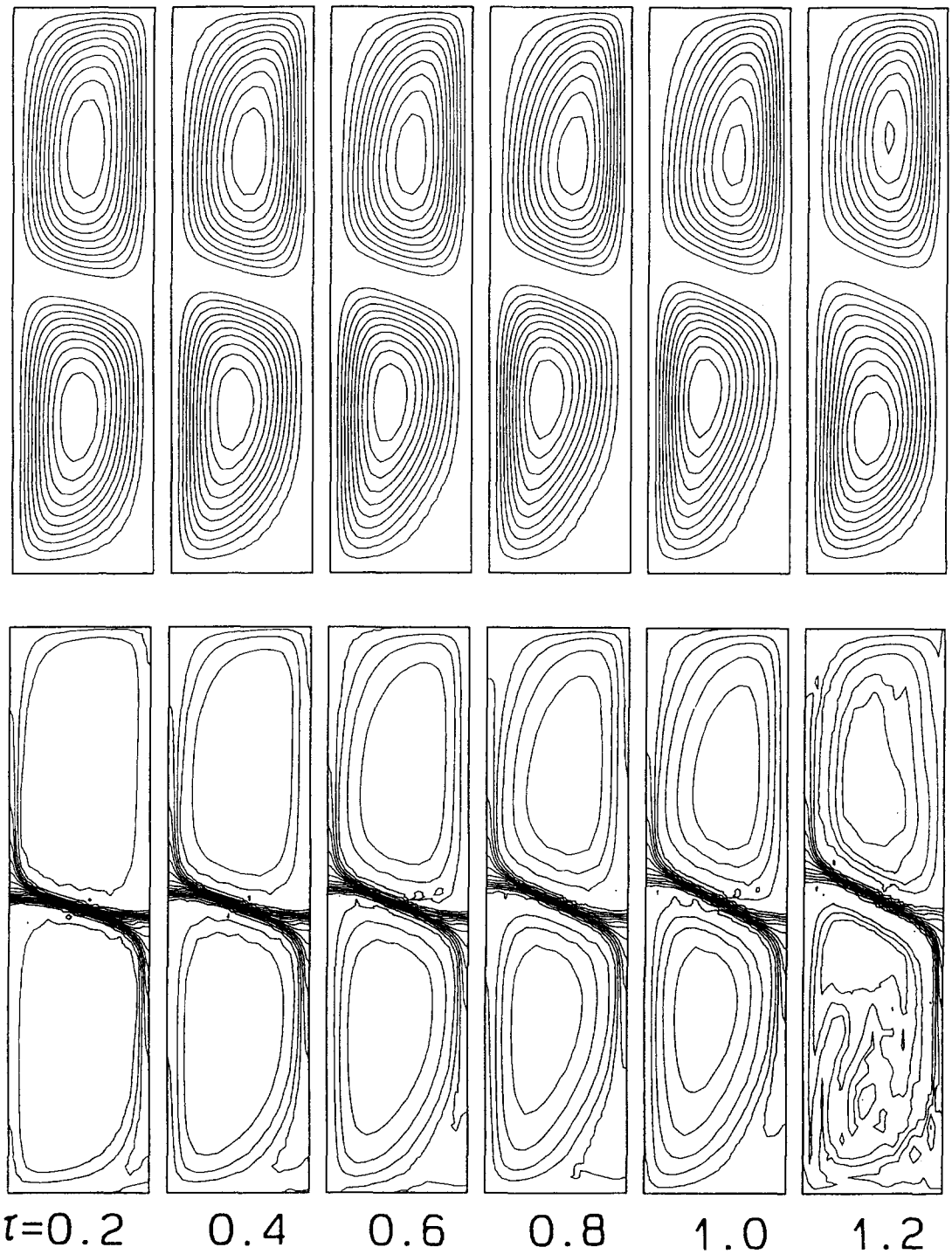

Fig. 5. Instantaneous contours of stream function (upper row), and concentration (lower row) in the case of the temperature dependence of α, ν and D (case 2) for $Pr_0 = 6$, $Le_0 = 100$, $A = 4$, $Ra_0 = 10^5$ and $N_0 = 2$. Iso-concentration lines are drawn by dividing the initial maximum concentration difference into 20 equal sections. (*Continued opposite.*)

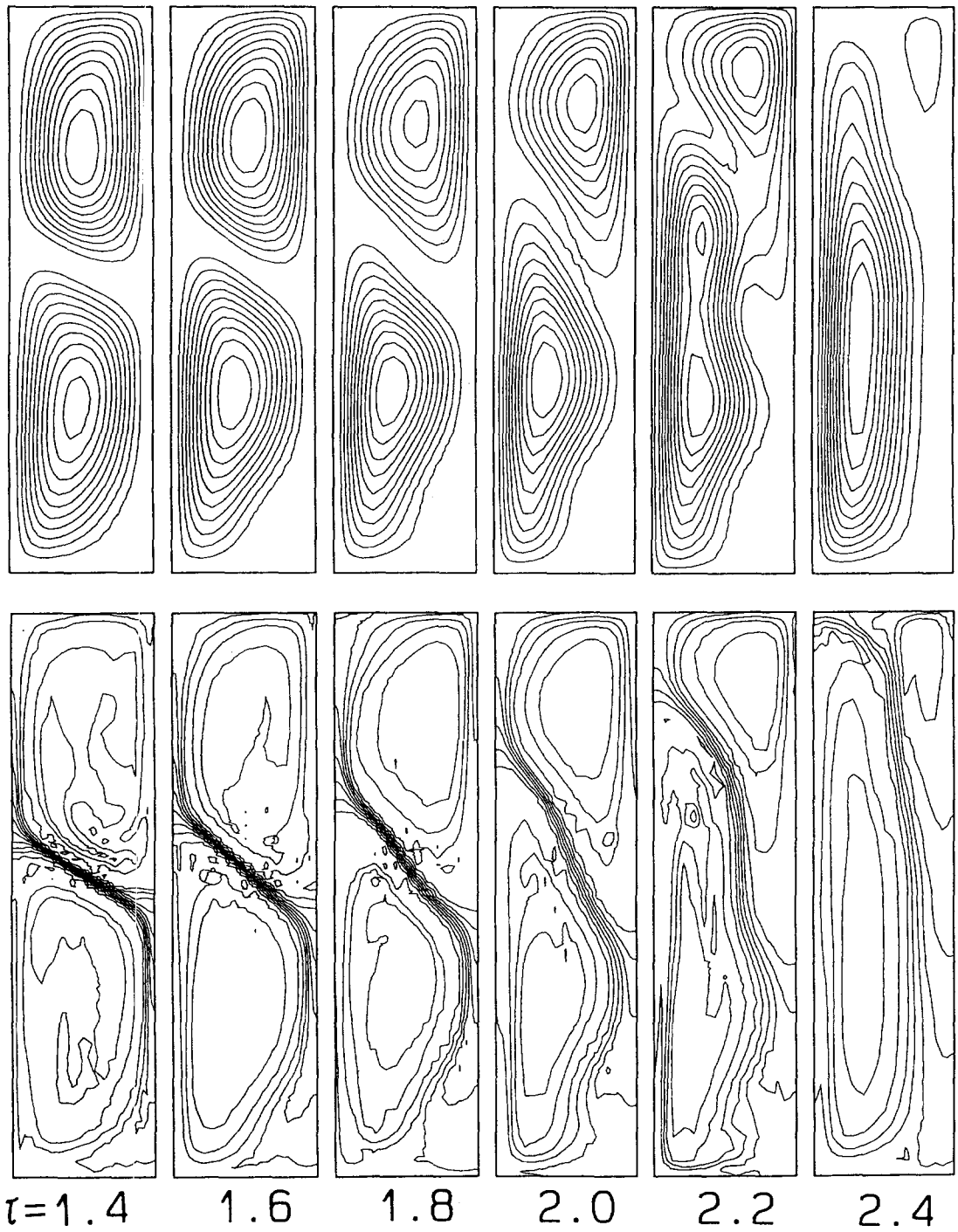

Fig. 5—*continued.*

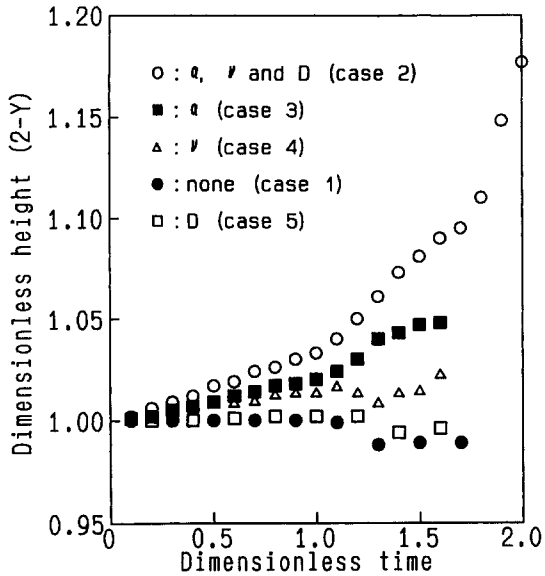

Fig. 6. Migration of the interface with the temperature dependence of properties of the fluid.

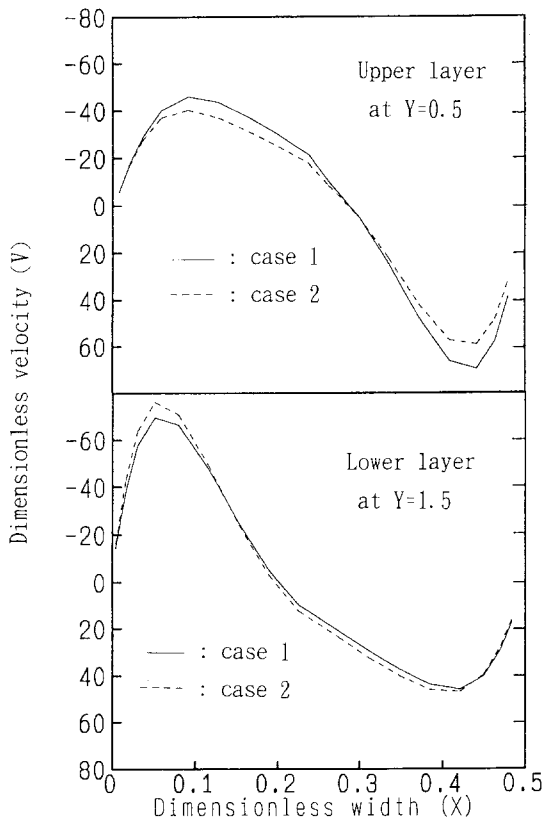

Fig. 7. Distribution of the dimensionless velocity in the Y-direction at $\tau = 0.8$.

layer being stronger than that along the cold wall in the upper layer.

REFERENCES

1. J. S. Turner and H. Stommel, A new case of convection in the presence of combined vertical salinity and temperature gradients, *Proc. U.S. Nat. Acad. Sci.* **52,** 49–53 (1964).
2. J. S. Turner, Double-diffusive phenomena, *A. Rev. Fluid Mech.* **6,** 37–56 (1974).
3. H. E. Huppert and J. S. Turner, Double-diffusive convection, *J. Fluid Mech.* **106,** 299–329 (1981).
4. C. F. Chen and D. H. Johnson, Double diffusive convection: a report on an engineering foundation conference, *J. Fluid Mech.* **138,** 405–416 (1984).
5. C. E. Mendenhall and M. Mason, The stratified subsidence of fine particles, *Proc. U.S. Natl Acad. Sci.* **9,** 199–202 (1923).

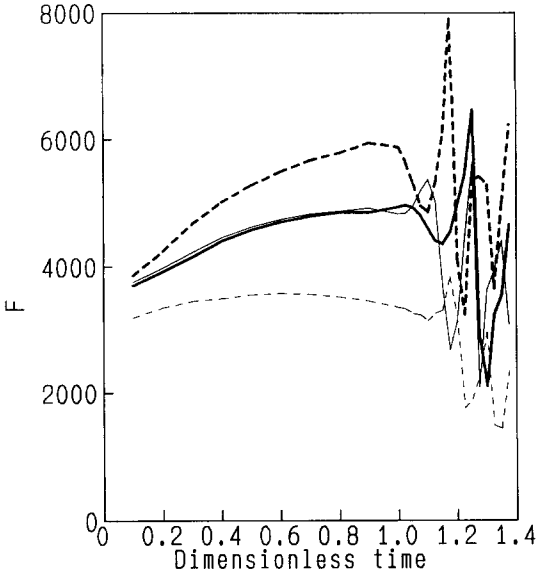

Fig. 8. Variation of dimensionless inertial force (F) in the Y-direction. Solid lines correspond to case 1 (no temperature dependence), and broken lines to case 2 (temperature dependence). The bold line is evaluated near the hot wall at $Y = 1.5$ (lower layer) and the fine line near the cold wall at $Y = 0.5$ (upper layer). The dimensionless inertial force was calculated for $\alpha = 0.000\,234\ \mathrm{K}^{-1}$, $\beta = 0.000\,64\ \mathrm{m}^3\ \mathrm{kg}^{-1}$, $\Delta T_{max} = 10$ K, $\Delta c_{max} = 10\ \mathrm{kg\ m}^{-3}$ and $N = 2$. The variation of F-values after $\tau = 1.0$ occurred as a result of characteristic oscillatory phenomena in double-diffusive natural convection [12].

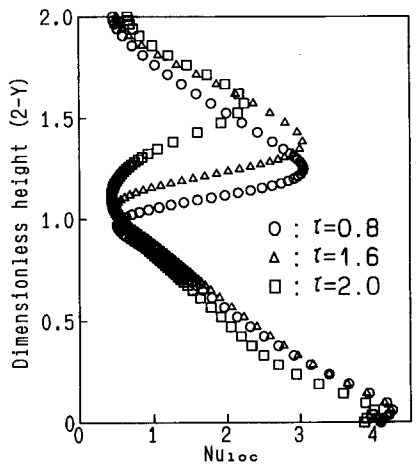

Fig. 9. Local Nusselt number on the hot wall with the temperature dependence of α, ν and D (case 2).

6. S. A. Thorpe, P. K. Hutt and R. Soulsby, The effect of horizontal gradients on thermohaline convection, *J. Fluid Mech.* **38,** 375–400 (1969).
7. K. Kamakura and H. Ozoe, Experimental and numerical analyses of double diffusive natural convection heated and cooled from opposing vertical walls with an initial condition of a vertically linear concentration gradient, *Int. J. Heat Mass Transfer* **36,** 2125–2134 (1993).
8. K. Kamakura and H. Ozoe, Double-diffusive natural convection between vertical parallel walls: numerical analyses for two-layer convection, *Proceedings 3rd ASME/JSME Thermal Engineering Joint Conference*, Vol. 1, pp. 141–146 (1991).
9. K. Kamakura and H. Ozoe, Double-diffusive natural convection in a two-layer system of large concentration difference, *Proceedings 1st International Conference Transport Phenomena in Processing*, pp. 720–730 (1993).
10. K. Kamakura and H. Ozoe, Double-diffusive natural convection between vertical parallel walls: experimental study on two-layer convection, *J. Chem. Engng Japan* **24,** 622–627 (1991).
11. K. Kamakura and H. Ozoe, Numerical analyses of transient formation and degradation process of multi-layered roll cells with double-diffusive natural convection in an enclosure, *Numer. Heat Transfer Part A* **23,** 101–117 (1993).
12. K. Kamakura and H. Ozoe, Oscillatory double diffusive natural convection in a two-layer system, *Proceedings 10th International Heat Transfer Conference*, Vol. 7, pp. 67–72 (1994).